Check for updates

Received: 27 July 2023 | Accepted: 8 August 2024

DOI: 10.1111/ivb.12439

ORIGINAL ARTICLE

Invertebrate Biology WILEY

Excitation–contraction coupling reflects the metabolic profile of mantle muscle in young cuttlefish (*Sepia officinalis*)

Neal I. Callaghan[1,2] | Loïck Ducros[3] | J. Craig Bennett[4] | Juan C. Capaz[5] | José Pedro Andrade[5] | Antonio V. Sykes[5] | William R. Driedzic[6] | Simon G. Lamarre[3] | Tyson J. MacCormack[7]

[1]Institute of Biomedical Engineering, Faculty of Applied Science and Engineering, University of Toronto, Toronto, Ontario, Canada

[2]Translational Biology and Engineering Program, Ted Rogers Centre for Heart Research, Toronto, Ontario, Canada

[3]Département de Biologie, Université de Moncton, Moncton, New Brunswick, Canada

[4]Department of Physics, Acadia University, Wolfville, Nova Scotia, Canada

[5]CCMAR, Centro de Ciências do Mar do Algarve, Campus de Gambelas, Universidade do Algarve, Faro, Portugal

[6]Department of Ocean Sciences, Memorial University of Newfoundland, St. John's, Newfoundland, Canada

[7]Department of Chemistry and Biochemistry, Mount Allison University, Sackville, New Brunswick, Canada

Correspondence
Simon G. Lamarre, Département de Biologie, Université de Moncton, Moncton, New Brunswick, Canada.
Email: simon.lamarre@umoncton.ca

Tyson J. MacCormack, Department of Chemistry and Biochemistry, Mount Allison University, Sackville, New Brunswick, Canada.
Email: tmaccormack@mta.ca

Funding information
NIC was supported by a Natural Sciences and Engineering Research Council of Canada (NSERC) Vanier Canada Graduate Scholarship and a Comparative Physiology and Biochemistry section travel grant from the Canadian Society of Zoologists. This work was supported NSERC Discovery operating grants to TJM, SGL, and WRD. AVS was supported by Fundação para a Ciência e a Tecnologia (FCT) through Programa Investigador FCT 2014 (IF/00576/2014). This study received Portuguese national funds in part to JPA's research group from Programa Operacional Regional do Centro Mar2020 (Portugal2020/FEAMP) - Project SEPIACUL (project number 16-02-01-FMP-53), from FCT through project UID/Multi/04326/2019, Plurennial funding to CCMAR (UID/Multi/04326/2016), and from the operational programmes CRESC Algarve 2020 and COMPETE 2020 through project

Abstract

The mantle muscle of common cuttlefish, *Sepia officinalis*, is responsible both for high-magnitude and rapid movements for locomotion, as well as sustained ventilation, which require specific metabolic, electrophysiological, and structural organization. Young cuttlefish have a highly oxidative phenotype and a rapid growth rate. Here, we show high rates of oxygen consumption and protein synthesis in juveniles, and these rates decay exponentially over the first few weeks of growth. This is associated with considerable citrate synthase activity (relative to larger cuttlefish) but a lack of glucose metabolism based on zero uptake of glucose by isolated muscle sheets and minimal activity of hexokinase (similar to larger animals). In contrast to glucose metabolism in the heart, glucose metabolism in these muscle sheets was not stimulated by extracellular taurine. Previous research revealed an unusual ion channel complement in mantle myocytes, the most notable feature of which is the lack of a Na^+ current during depolarization. Because this adaptation is not consistent across the coleoid clade, we investigated excitation–contraction coupling. Here, mantle energetics and contractility, including the individual components of the total Ca^{2+} flux driving contraction, were studied. Results indicate that the majority of Ca^{2+} current underlying contractile stress development capacity in cuttlefish juveniles is not mediated by dihydropyridine-sensitive L-type channels, in contrast to their adult counterparts, and the sarcoplasmic reticulum contributes little to routine contractility. We had previously noted an influence of physiological levels of taurine in limiting cardiac

Simon G. Lamarre and Tyson J. MacCormack contributed equally to the work.

This is an open access article under the terms of the Creative Commons Attribution-NonCommercial License, which permits use, distribution and reproduction in any medium, provided the original work is properly cited and is not used for commercial purposes.
© 2024 The Author(s). *Invertebrate Biology* published by Wiley Periodicals LLC on behalf of The American Microscopical Society LLC.

EMBRC.PT ALG-01-0145-FEDER-022121. This study also received support from the Portuguese node of EMBRC-ERIC, specifically EMBRC.PT ALG-01-0145-FEDER-022121. WRD held the Canada Research Chair in Marine Bioscience. The Microscopy Unit at UAlg where fluorescence microscopy was performed was partially supported by national Portuguese funding FCT: UID/BIM/04773/2013 CBMR and PPBI-POCI-01-0145-FEDER-022122.

contractility but found no analogous sensitivity in mantle muscle. Finally, transmission electron microscopy of subcellular architecture revealed the presence of sarcoplasmic tubular aggregates, suggesting that oxidative inhibition of sarcoplasmic reticulum function limits its role in this life stage.

KEYWORDS
calcium flux, excitation–contraction coupling, glucose uptake, metabolic enzymes, muscle, oxygen consumption, sarcoplasmic reticulum, taurine, tubular aggregates

1 | INTRODUCTION

Cephalopods, including the common cuttlefish (*Sepia officinalis* LINNAEUS 1758), mobilize extensively using jet propulsion. This method of locomotion is especially critical during escape activity and in young animals that are mechanically disadvantaged in undulatory mantle fin-enabled swimming (Bartol et al., 2008, 2009; Staaf et al., 2014). Accordingly, the biomechanics of jet propulsion are optimized for animal size and behavior (Gladman & Askew, 2022). The current study examines metabolism and mechanical function in mantle muscle of juvenile (0.5–3 g; Vidal & Shea, 2023) cuttlefish. Young cuttlefish can grow at rates as high as 12% body weight per day (Sykes et al., 2014), devoting at least 41% of whole animal oxygen consumption to mantle protein synthesis (Fraser & Rogers, 2007; Lamarre et al., 2019). Mantle muscle displays a highly oxidative phenotype and a remarkable relative growth rate, suggesting a highly specialized metabolic phenotype in juvenile animals (Lamarre et al., 2016, 2019; Speers-Roesch et al., 2016). In isolated mantle muscle, following a simulated jetting event, the rate of protein synthesis increases by 24% and is accompanied by a 29% increase in oxygen consumption. Inhibition of glucose metabolism results in a 50% decrease in protein synthesis and oxygen consumption, indicating a necessity for glucose metabolism. Despite this, there was no change in glucose uptake immediately following the activity period associated with the increase in protein synthesis and oxygen consumption (Lamarre et al., 2019). Glucose metabolism is stimulated by extracellular taurine in cuttlefish systemic heart (MacCormack et al., 2016), but it is unclear whether this is the case for other tissues. Here, we assess whether extracellular taurine is a requirement for glucose uptake in mantle muscle. In addition, we report the scaling of activity of key enzymes in energy metabolism with body mass to determine how the metabolic phenotypes of young cuttlefish change with growth. We specifically focused on hexokinase, which catalyzes the first intracellular reaction in glucose utilization; citrate synthase, which is an indicator of aerobic potential; and octopine dehydrogenase, which catalyzes the terminal step in anaerobic metabolism.

The mantle of coleoid (soft-bodied) cephalopods represents a powerful physiological model in which to study muscle contractility, as it is responsible both for acute high-pressure jetting events as well as sustained low-pressure ventilatory movements (Gladman & Askew, 2022; Packard & Trueman, 1974; Trueman & Packard, 1968). Despite apparent similarities in body form and mantle function in coleoids, the cellular physiology of the mantle muscle diverges considerably between orders. Electrophysiologically, for example, squid in the genus *Alloteuthis* have rapid all-or-nothing action potentials (APs) carried mainly by the Na^+ current, which seem pervasive across the mantle because a given stimulation current can induce the same relative force production across different tissue thicknesses (Rogers et al., 1997). This organization is rather traditional in the context of comparative physiology and reflects the squid's niche as a pelagic hunter, which requires both swimming speed and endurance. In contrast, the relatively sessile adults in the octopus genus *Eledone* and of the common cuttlefish (*S. officinalis*), both of which rely on ambush hunting in a benthic setting, seem to have no Na^+ component to their mantle APs. Instead, their AP current is virtually ablated upon L-type Ca^{2+} channel (LTCC) blockade (Rogers et al., 1997). Squid and cuttlefish are in the superorder Decapodiformes, whereas octopus comprise the Octopodiformes. Accordingly, such niche-specific differences in muscle physiology raise interesting questions concerning the convergent evolution of, or selective loss of, a Na^+ current component to the AP, as well as the energetics supporting its function. Understanding the basis for such fundamental differences in excitation–contraction (E–C) coupling may provide valuable insights into the physiological and energetic advantages and disadvantages of each model.

The obliquely striated mantle muscle of cephalopods more closely resembles mammalian cardiac muscle than skeletal muscle, in both functional structure and molecular derivation (Zullo et al., 2017); coleoid muscles possess cardiac-like dyadic structures instead of the triads of mammalian skeletal muscle (Feinstein et al., 2011), and they rely on peripheral coupling processes instead of t-tubules (Kier, 1985). Mature coleoid striated muscle also contains a rudimentary sarcoplasmic reticulum (SR) (Feinstein et al., 2011; Kier, 1985); however, little is known about its capacity or activity. The SR of coleoid systemic heart muscle is well developed and plays an important role in Ca^{2+} cycling on a beat-to-beat basis (Altimiras et al., 1999; Gesser et al., 1997), but the SR's significance in striated muscle function has been poorly studied. The regulation of intracellular Ca^{2+} is particularly important in cephalopods because of the relatively high concentration of Ca^{2+} in their hemolymph, ~10.5 mmol/L compared to the ~2 mmol/L of most vertebrates. MacCormack et al. (2016) have shown that extracellular taurine, the most abundant free amino acid in cuttlefish blood, plays an important role in controlling contractility and protecting systemic and branchial heart muscle from high extracellular Ca^{2+} (Ca^{2+}_e) levels. In vertebrate skeletal muscle, intracellular Ca^{2+} (Ca^{2+}_i) accumulation can activate a variety of pathways that result in cellular damage and loss of function (Gissel, 2005). In mammalian fast-twitch muscle,

17447410, 2024, 3, Downloaded from https://onlinelibrary.wiley.com/doi/10.1111/ivb.12439 by Universidade Do Algarve, Wiley Online Library on [06/11/2024]. See the Terms and Conditions (https://onlinelibrary.wiley.com/terms-and-conditions) on Wiley Online Library for rules of use; OA articles are governed by the applicable Creative Commons License

chronic disruptions in $Ca^{2+}{}_i$ regulation can also trigger the misfolding and inactivation of SR Ca^{2+} ATPase proteins (SERCA), with the subsequent formation of SR membrane-derived tubular aggregates (Boncompagni et al., 2012). It is possible that extracellular taurine may serve a similar role in preventing $Ca^{2+}{}_i$ accumulation in cuttlefish mantle muscle, but this has yet to be investigated.

The goal of the current study was to characterize metabolism and functional aspects of E–C coupling in mantle muscle of very young (e.g., <3 g) cuttlefish with a specific focus on metabolic phenotyping and Ca^{2+} flux. A nonlinear relationship between animal body mass and oxygen consumption/protein synthesis was demonstrated amid constant specific activities of key enzymes of central carbon metabolism, suggesting extreme metabolic demands in young animals. Isometrically contracting mantle muscle preparations were employed to characterize mantle contractile endurance and the relative contributions of LTCC and SR in twitch and tetanic force production. Given its seemingly critical role in heart muscle, the contribution of extracellular taurine to the regulation of glucose uptake and mantle muscle contractility was also assessed. Finally, the ultrastructural anatomy of mantle myocytes from cuttlefish was examined to support pharmacological findings and to compare metabolic features with existing literature on adults of the same species and the life histories of other cephalopods. Our results indicate that E–C coupling mechanisms and the subcellular architecture of mantle myocytes substantially differ between young and adult cuttlefish; potential reasons for these differences are discussed. When considered in concert with their fast muscle cycling (Gladman & Askew, 2022), the early life stage of the cuttlefish represents an ideal model in which to examine the intersection of unusual muscle electrophysiological and metabolic organization to produce a highly successful organism.

2 | METHODS

2.1 | Ethical statement

All the procedures were approved by CCMAR Animal Welfare Committee (ORBEA CCMAR-CBMR) and Direcção-Geral de Alimentação e Veterinária (DGAV) of the Portuguese Government, according to National (Decreto-Lei 113/2013) and EU legislation (Directive 2010/63/EU) on the protection of animals used for scientific purposes. In addition, protocols were approved by institutional Animal Care Committees at Université de Moncton (UdeM-18-02) and Memorial University of Newfoundland. Procedures were only applied to live animals by authorized users.

2.2 | Animals and tissue sampling

Cuttlefish (*S. officinalis*) of an F2 captive stock were reared at CCMAR's Ramalhete Aquaculture Station (Ria Formosa, Portugal, 37°00′22.39″N; 7°58′02.69″W) in a 1,500-L round, black fiberglass tank with an open seawater system, according to methods of Sykes et al. (2014). Both temperature and dissolved oxygen (DO_2) were measured with a VWR DO220 probe, and salinity was measured with a VWR EC300 salinity meter. Water temperature was 20.8 ± 1.14°C (mean ± *SD*), salinity was 34.6 ± 0.71 g/l, and DO_2 was 101.0 ± 1.60% air saturation. Post-hatch juveniles were fed live mysids, and once the juveniles reached mass >1.5 g, they were fed live grass shrimp (*Palaemon varians*), both ad libitum on a daily basis. Animal mass in biochemical studies is shown in Section 3. Animals used in contractile studies were 6–8 weeks after hatching, with a mass of 1.1 ± 0.04 g (mean ± *SEM*; $n = 28$). Following the guidelines for care and welfare of cephalopods (Fiorito et al., 2015), cuttlefish were euthanized for sampling of the ventral mantle tissue in 0.22 µm-filtered seawater (FSW) containing 10% EtOH. After animals became unresponsive, stopped ventilation, and chromatophore activity ceased (~2 min), death was confirmed by cerebral bisection and decapitation (Lewbart & Mosley, 2012).

2.3 | Whole-animal respirometry

Whole-animal resting aerobic metabolic rate ($\dot{M}O_2$) was measured in animals 9 days, 1 month, and 2 months of age ($n = 6$ per age) by use of custom-made respirometry chambers. Briefly, the chamber consisted of a cylindrical plastic container equipped with a tight-fitting lid on which a rubber port was installed to accommodate a 3-mm fiber-optic oxygen sensor (Robust Oxygen Sensor, PyroScience GmbH, Aachen DE). A false bottom allowed for gentle water agitation using a magnetic stir bar operated at very low speed. For the smaller animals (up to 1 month old), the assembled chamber volume was 87.5 ml, whereas the larger animals (2 months old) were studied in a chamber with a volume of 348 ml. The animals were gently placed in the chamber, and the lid was fitted while completely immersed in water to avoid trapping air in the respirometer. Animals were allowed to acclimate for 30 min following introduction to the chamber prior to measurement. Oxygen concentration was then measured at 1 Hz for 1 h using a FireSting-O2 and recorded using Pyro Oxygen Logger (PyroScience GmbH). At 20-min intervals, the water in the chamber was gently replaced by immerging the chamber in fresh aerated seawater at the same temperature. Oxygen concentration was always above 80% air saturation during the trials. For each animal, three slopes of oxygen concentration in relation to time were obtained ($R^2 > .95$), averaged, and normalized to body mass to calculate $\dot{M}O_2$. Background respiration rate, measured in an empty chamber, was subtracted from the calculated $\dot{M}O_2$. The results are presented in µmol $O_2\ g^{-1}\ h^{-1}$.

2.4 | Mantle protein synthesis measurement

The fractional rate of protein synthesis (*Ks*) in mantle was determined following a modified version of the flooding dose method (Garlick et al., 1980; modified by Lamarre et al., 2015). Cuttlefish between 3 days and 2 months old and weighing between 107 and 2,785 mg ($n = 24$) were transferred into a 6-L tank containing

17447410, 2024, 3, Downloaded from https://onlinelibrary.wiley.com/doi/10.1111/ivb.12439 by Universidade Do Algarve, Wiley Online Library on [06/11/2024]. See the Terms and Conditions (https://onlinelibrary.wiley.com/terms-and-conditions) on Wiley Online Library for rules of use; OA articles are governed by the applicable Creative Commons License

aerated seawater supplemented with 0.75 mM phenylalanine (PHE) and 0.75 mM deuterated phenylalanine ([D_5]-PHE, ring-D5-phenylalanine, Cambridge Isotope Laboratories Inc., Tewksbury, MA, United States) maintained at ~21°C. After an incubation period of 90 min, cuttlefish were quickly euthanized, mantles collected, gently blotted dry, and flash-frozen in liquid nitrogen. The rate of protein synthesis was then measured as described in Lamarre et al. (2019); briefly, samples were homogenized in 0.2 mol/L perchloric acid, hydrolyzed in 6 mol/L HCl, subjected to solid phase extraction, derivatized with pentafluorobenzyl bromide, and analyzed by gas chromatography and mass spectrometry. The fractional rate of protein synthesis is presented as the percentage change in protein content per day.

2.5 | Tissue glucose uptake and enzyme activities

Following euthanasia, a cut was made up the center of the ventral side of the mantle. The mantle was splayed open, one wing was isolated, and skin was carefully removed by dissection with a blunt probe. The mantle tissue was incubated in FSW containing 1 mmol/L glucose with either no further addition or supplemented with either 100 mmol/L taurine or 100 mmol/L sucrose. The tissue to medium ratio was 1 g to 9 ml (e.g., 0.01 g tissue plus 90 µl medium). Isolated tissue was incubated for 1 h with gentle shaking. Thereafter, glucose concentration in the medium was analyzed in buffer containing 250 mmol/L imidazole, 5.0 mmol/L $MgSO_4$, 10 mmol/L ATP, 0.8 mmol/L $NADP^+$, excess glucose-6-phosphate dehydrogenase, and thereafter treated with excess hexokinase. A standard curve was created for glucose analysis. Assays were conducted in a BioTek Synergy HT microplate reader (Agilent, Santa Clara, CA, United States) at a wavelength of 340 nm.

For enzyme activity studies, tissue was flash-frozen at sampling and then homogenized as previously described (Lamarre et al., 2016). Enzyme activity of octopine dehydrogenase (ODH) was assayed in buffer containing 50 mmol/L imidazole (pH 7.4), 1.0 mmol/L KCN, 0.2 mmol/L NADH, 4.0 mmol/L pyruvate, and 10 mmol/L L-arginine (omitted for control), and absorbance was monitored at 340 nm. Hexokinase (HK) activity was assayed in buffer containing 50 mmol/L imidazole buffer (pH 7.4), 5.0 mmol/L $MgCl_2$, 1.0 mmol/L glucose, 0.4 in mmol/L $NADP^+$, 2 U/ml glucose-6-phosphate dehydrogenase, and 2.0 mmol/L ATP (omitted for control), and absorbance was monitored at 340 nm. Citrate synthase (CS) activity was measured as previously described (Speers-Roesch et al., 2016). The chymotrypsin-like activity of the 20S proteasome was also measured using a microplate-based fluorescence assay (Shibatani & Ward, 1995), as per Lamarre et al. (2012, 2016). Tissue incubations and enzyme activities were determined at a controlled room temperature (~21°C).

2.6 | Isometrically contracting mantle strip preparations

Mantle tissue samples from animals >1.5 g were used for paired twitch mechanics analysis under several conditions. With a fresh razor blade, paired, circumferentially oriented sections ~8 mm long, 2 mm wide, and full thickness were cut from the anterior lip of the ventral mantle, and the skin was carefully removed by dissection with a blunt probe. In previous experiments on cuttlefish and other model organisms, small molecules and pharmacological agents, including taurine and ryanodine, can rapidly affect function in muscle preparations of this thickness (Henry & MacCormack, 2017; Lamarre et al., 2019; MacCormack et al., 2016).

Freshly isolated mantle strips were attached to calibrated isometric force transducers (model 60-2994, Harvard Apparatus, South Natick, MA, United States) by short 6-0 silk sutures and clamped inside double-walled 20-ml experimental chambers containing static FSW (Lowy & Millman, 1962; MacCormack et al., 2016) with 1.0 mmol/L glucose (Capaz et al., 2017), maintained at 20.0 ± 0.01°C. Transducers were interfaced to a PowerLab 8/35 data acquisition system, and data were recorded using LabChart 8 software (ADInstruments, Colorado Springs, CO, United States). Strips were then gently stretched (<5%) under sporadic field excitation by paired 1.2-mm platinum electrodes with an SD9 (Grass Technologies Inc., Warwick, RI, United States) physiological stimulator (100 V, 5 ms duration) until peak isometric stress was achieved (Milligan et al., 1997). All experiments were conducted within 45 min of isolation.

2.6.1 | Experiment 1: Force-frequency relationship

One subset of mantle muscle preparations ($n = 8$, all from different animals) was used to assess contractility responses to increasing stimulation frequencies. After mounting in the apparatus, preparations were allowed to rest and equilibrate for 10 min, before being subjected to 15 square wave pulses (100 V, 5 ms duration) at increasing frequencies, starting at 0.2 Hz. Stimulation frequency was progressively increased to 1.0 Hz in 0.2 Hz increments, with a 30 s rest period without stimulation between each increment.

2.6.2 | Experiment 2: Functional estimates of Ca^{2+} flux

A separate set of mantle strips was used to pharmacologically characterize the contribution of L-type Ca^{2+} channels and SR Ca^{2+} cycling to contractility. After preparations were established ($n = 6$ paired trials per treatment), one of two randomly selected parallel preparations was treated with 40 µl DMSO, and the other with either ryanodine (10 µmol/L final concentration) (Gesser et al., 1997) or nifedipine (10 µmol/L final concentration) (Milligan et al., 1997) in 40 µl DMSO. Preparations were allowed to rest and equilibrate for 10 min before being subjected to six square wave pulses (100 V, 5 ms duration) at 0.2 Hz. After a 2 min rest, preparations were stimulated with the same waveform at 50 Hz to generate a tetanic contraction, which was maintained until they had dissipated >90% of peak contractile force, to allow for the detection of small Ca^{2+} handling differences between treatments.

17447410, 2024, 3, Downloaded from https://onlinelibrary.wiley.com/doi/10.1111/ivb.12439 by Universidade Do Algarve, Wiley Online Library on [06/11/2024]. See the Terms and Conditions (https://onlinelibrary.wiley.com/terms-and-conditions) on Wiley Online Library for rules of use; OA articles are governed by the applicable Creative Commons License

A rapid cooling protocol was also used to stimulate Ca^{2+} release from the SR. Rapid cooling to below 5°C triggers Ca^{2+} release from the SR in skeletal and cardiac muscle preparations from vertebrates (Konishi et al., 1985). Tension generation during such rapid cooling contractures (RCC) is proportional to the concentration of Ca^{2+} released and can be used to estimate the magnitude of SR Ca^{2+} stores (Bers, 1989; Talon et al., 2000). Mantle muscle preparations ($n = 4$) were established at 20.0°C as described in Experiment 1 and were not stimulated at any point following initial setup and stretching to optimal tension development. Following the 10-min acclimation period, the bathing media in the chamber was rapidly drained and immediately (<2 s) replaced with ice-cold media of identical composition. Muscle tension was continuously monitored throughout the procedure.

2.6.3 | Experiment 3: Influence of taurine on contractility

A final set of mantle strips was employed to determine whether extracellular taurine influenced contractility. Preparations ($n = 7$ paired trials per treatment) were established and experiments carried out as described in Experiment 2, except that one of two randomly selected parallel preparations was treated with 100 mmol/l taurine and the other with an equivalent concentration of sucrose to maintain constant osmolality between treatments (MacCormack et al., 2016).

2.7 | Isolation and Ca^{2+} imaging of mantle myocytes

Animals ($n = 5$) were sampled for paired taurine or sucrose exposure and Ca^{2+} imaging. Immediately following euthanasia, the lower mantle was dissected, minced to pieces of 1 mm or less in each dimension, and gently but regularly triturated using a 1 ml wide-bore pipette in FSW containing 2.5 mg/ml Type 2 collagenase (Worthington Biochemical Corporation, Lakewood, NJ), 1.0 mmol/L glucose and 100 mmol/L taurine for ~20 min. The resulting crude isolate was passed through a 70 µm nylon net filter and then centrifuged at 400*g* for 45 s. The supernatant was removed, and the pellet gently resuspended in FSW with 1.0 mmol/L glucose and 100 mmol/l taurine, then plated on glass slides that had previously been washed with 1 mmol/L NaOH, incubated in 20 mg/ml gelatin in FSW for 1 h, and then rinsed with FSW. Cells were left to attach for 30 min and rinsed with FSW before viability was assessed using a final concentration of 0.2% (w/v) Trypan Blue. Cells were examined with an optical microscope under a 40X objective and imaged with a Dino-Eye AM4023X 1.3 MP digital eyepiece camera (AnMo Electronics Corporation, New Taipei City, Taiwan). To examine taurine-dependent intracellular Ca^{2+} flux, cells were then incubated for 1 h at room temperature in a Ringer's solution containing 458 mmol/L NaCl, 4.89 mmol/L $MgSO_4$, 52.7 mmol/L $MgCl_2{\cdot}6\ H_2O$, 23.8 mmol/L KCl, and 3.38 mmol/L $NaHCO_3$ (pH 7.6) (MacCormack et al., 2016), to which was added either 100 mmol/L taurine or 100 mmol/L sucrose. Fluo-4 AM (Thermo-Fisher Scientific, Waltham, MA, United States) DMSO stock was spiked into the treatment medium for the last 30 min at a final concentration of 5 µmol/L. We used an SD9 stimulator to pace cells at 1 Hz, 5 ms duration, 50 V for 6 s on custom-made glass slides, coated as described above, with integrated carbon electrodes. Regions of interest containing fluorescing cells were visualized with an LSM710 microscope with a 488 nm excitation laser. Normalized Ca^{2+}-associated fluorescence was then compared between taurine and sucrose treatments.

2.8 | Transmission electron microscopy

Fresh mantle samples of similar size to those used for contractile preparations ($n = 2$ animals) were glutaraldehyde-fixed, stored at 4°C in fixative for ~1 month, and then post-fixed in 1% OsO_4 in PBS for 2 h. Samples were dehydrated in EtOH steps, followed by pure acetone. Epon 812 resin was used in 33%, 66%, and 100% steps for infiltration. Polymerization was carried out overnight at 60°C. Sections 80–100 nm thick were taken from the embedded samples and stained with saturated aqueous uranyl acetate (30 min) and Reynold's lead citrate (2 min). Sections were examined at an accelerating voltage of 150 kV with a CM30 TEM (Philips Electron Optics, Eindhoven, the Netherlands).

2.9 | Data analysis and statistics

The relationships between animal mass and $\dot{M}O_2$, rate of protein synthesis, and enzyme activity were analyzed using linear and nonlinear regressions. For glucose uptake experiments, statistical significance was assessed with a one-sample *t* test to compare the mean value to an expected value of 1. For isometrically contracting mantle muscle preparations, stress (in mN/mm^2) was calculated according to Shiels et al. (2010), assuming a muscle density of 1.06 g/cm^3 (Dabrowski, 1978; Layland et al., 1995). Stress traces were analyzed for resting and net maximum values, integrated contractile stress over time, tetanus:twitch maximum stress ratios, and times to peak stress and half relaxation from both twitch and tetanic traces. The use of two simultaneous mantle strip preparations from the same animal allowed for paired pharmacological manipulation (ryanodine or nifedipine vs. DMSO sham). All analyses were carried out using Prism 9 (GraphPad Software Inc., La Jolla, CA, United States). Pairwise treatments were tested for normality using the D'Agostino–Pearson omnibus test. Statistical significance was determined by paired *t* test, with significance set at $\alpha = .05$. Unless otherwise specified, data are presented as mean ± *SEM*.

3 | RESULTS

This study identifies links between metabolic capacity and E–C coupling function in juvenile cuttlefish. We chose to examine metabolic

17447410, 2024, 3, Downloaded from https://onlinelibrary.wiley.com/doi/10.1111/ivb.12439 by Universidade Do Algarve, Wiley Online Library on [06/11/2024]. See the Terms and Conditions (https://onlinelibrary.wiley.com/terms-and-conditions) on Wiley Online Library for rules of use; OA articles are governed by the applicable Creative Commons License

metrics by whole-body mass to better appreciate phenotypic changes that may arise dramatically over early life stages. Rates of oxygen consumption and protein synthesis were measured in intact animals. Isolated mantle sheets were used to assess the impact of size and taurine on glucose uptake, and mantle muscle samples were homogenized for characterization of metabolic enzyme activity. Animal $\dot{M}O_2$ declined with increasing mass (regression coefficient $p = .014$; Figure 1A), coinciding with decreased rates of mantle protein synthesis (*Ks*; regression coefficient $p < .0001$; Figure 1B). Glucose uptake from the medium could not be detected under any condition of mantle tissue incubation. This included incubation in FSW without any additions, incubation with either sucrose or taurine in the medium, or across a range of body masses (Table 1). The specific activity of ODH slightly increased with mass, whereas HK activity decreased with mass (regression coefficients $p = .0005$ and $p = .041$, respectively; Figure 2A,B); S and proteasome activity remained consistent across animal masses (regression coefficients $p = .45$ and $p = .55$ respectively; Figure 2C,D).

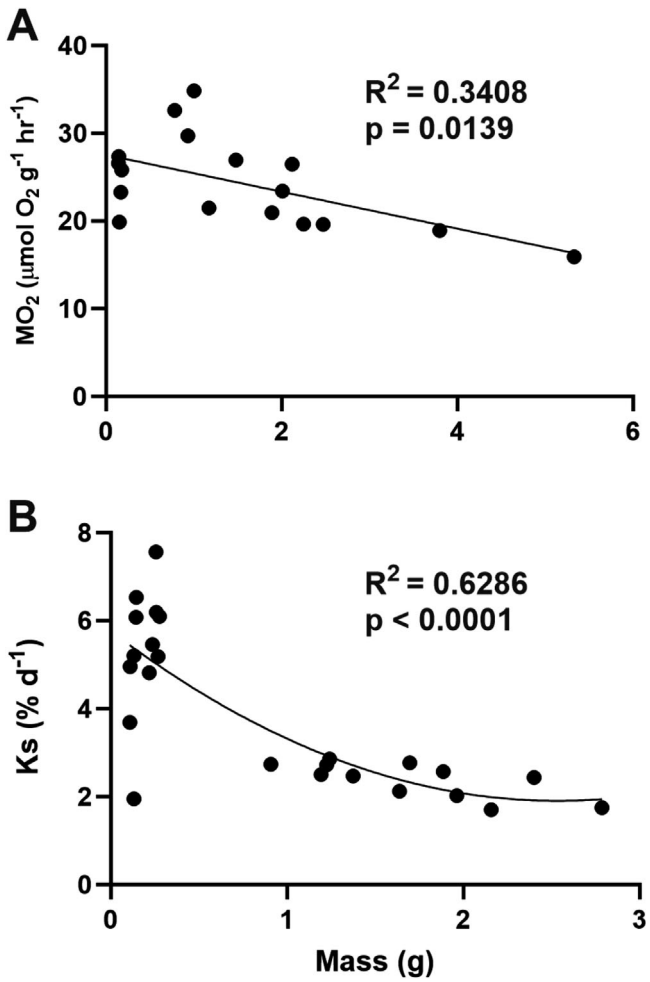

FIGURE 1 Whole-animal rates of oxygen consumption and protein synthesis in young cuttlefish (*Sepia officinalis*). (A) Whole-body rate of oxygen consumption ($\dot{M}O_2$) by whole-body mass. Linear regression is significantly different from zero. (B) Fractional rate of whole-animal protein synthesis (*Ks*) by body mass.

Isometrically contracting circumferential mantle strips from juveniles of *S. officinalis* were assessed for twitch stress production in the presence of specific inhibitors of SR function (ryanodine) and the LTCC current (nifedipine) (Figure 3); ryanodine inhibits the ryanodine receptor allowing Ca^{2+} release from the SR, whereas nifedipine inhibits L-type Ca^{2+} channels. Preparations were viable for several hours in the specified conditions, providing they were allowed rest between bouts of contraction. Contractile curve characteristics were similar in 0.2% (v/v) DMSO-treated sham preparations and paired preparations treated with either 10 µmol/L ryanodine or 10 µmol/L nifedipine ($n = 6$ each, Figure 3A). The mantle strips could maintain contractions at the imposed stimulation rate to >10 Hz before any summation was observed and continued to match the stimulation rate up to ~25 Hz with summation. The mantle muscle preparations exhibited a negative force–frequency relationship that reached steady state in net peak force at 70–80% peak stress (Figure 3B). Samples showed high cross-sectional peak contractile stress (117 ± 62 mN/mm^2, Figure 3C), although this is an underestimate of peak fiber stress because orthogonal or antagonistic fibers would also be included in the cross-sectional area of the fibers in this preparation, compared to thinner preparations used in other studies (e.g., Rogers et al., 1997). The second contraction in a 0.2 Hz stimulation train showed significantly lower time-integrated stress (impulse per unit cross-sectional area) compared to the initial contraction (paired *t* test, Figure 3D, $p = .0025$) because of a lower peak stress, demonstrating a slow refractory rate. Further analysis of single twitch kinetics and dynamics revealed no effect of 10 min incubation in 10 µmol/L ryanodine (Figure 3E,G,I,K) or nifedipine (Figure 3F,H,J,L) relative to their respective paired DMSO shams. There were no significant differences between control and pharmacologically treated preparations in peak stress (paired *t* tests, Figure 3E, ryanodine, $p = .68$; Figure 3F, nifedipine, $p = .75$), time-integrated stress (paired *t* tests, Figure 3G, ryanodine, $p = .15$; Figure 3H, nifedipine, $p = .45$), time to peak tension (paired *t* tests, Figure 3I, ryanodine, $p = .21$; Figure 3J, nifedipine, $p = .91$), or time from peak to half-peak relaxation (paired *t* tests, Figure 3K, ryanodine, $p = .20$; Figure 3L, nifedipine, $p = .48$). In an effort to release SR Ca^{2+} stores, a cold-shock experiment was carried out in which the bathing medium at 20.0°C was rapidly replaced with ice-cold medium in the absence of any electrical stimulation. All preparations maintained consistent baseline resting tensions and showed no evidence of RCC following this treatment (data not shown).

Although we were unable to determine a ryanodine-sensitive (SR) or nifedipine-sensitive (LTCC) contribution to mantle muscle contractility, we noted beat-to-beat sensitivity and strong frequency dependence of single-twitch stress. To further elucidate the contributors to E–C coupling, we subjected the preparations to a physiological extreme in the form of tetanic contractions (Lowy & Millman, 1962; Rosenbluth et al., 2010). Stimulation of isometric mantle preparations above ~25 Hz induced an essentially tetanic contraction, and in this study, we used 50 Hz to elicit reproducible tetanic stresses. However, small unfused contractions were still noted at ~25 Hz (Figure 4A), suggesting the possible presence of multiple, physiologically distinct muscle types in the preparation. Neither ryanodine (paired *t* test,

17447410, 2024, 3, Downloaded from https://onlinelibrary.wiley.com/doi/10.1111/ivb.12439 by Universidade Do Algarve, Wiley Online Library on [06/11/2024]. See the Terms and Conditions (https://onlinelibrary.wiley.com/terms-and-conditions) on Wiley Online Library for rules of use; OA articles are governed by the applicable Creative Commons License

TABLE 1 Glucose concentration following incubation of isolated mantle muscle for 1 h in media initially containing 1.0 mmol/L glucose.[a]

Additions to media	Animal wet weight (g)	Glucose (mmol/L)
None	0.33 ± 0.031	0.99 ± 0.03
Taurine	0.16 ± 0.01	0.96 ± 0.05
Taurine	0.47 ± 0.02	1.00 ± 0.04
Taurine[b]	0.76 ± 0.12	0.99 ± 0.03
Sucrose[b]	0.76 ± 0.12	0.99 ± 0.03

[a]Sheets of mantle muscle were incubated for 1 h in filtered sea water with or without sucrose (100 mmol/L) or taurine (100 mmol/L). Initial concentration of glucose in all preparations was 1.0 mmol/L. $n = 6$ in all cases except group with mass of 0.47, for which $n = 11$. Final glucose concentration in all cases was not significantly different from 1.0 mmol/L.
[b]Tissue preparation from the same animal used for both incubation with taurine and sucrose.

Figure 4B, $p = .80$) nor nifedipine (paired t test, Figure 4C, $p = .89$) significantly affected the ratio between maximal contractile stresses during tetanus and a single twitch. Ryanodine treatment did not influence the shape of the tetanic curve, although there was bimodal response consisting of delayed time to peak tetanic stress in two of the samples tested (Figure 4D), with no clear effect on the other four; however, this pattern was not statistically significant (paired t test, $p = .59$). Application of nifedipine significantly reduced the time from peak to half-peak tetanic stress (paired t test, Figure 4E, $p = .006$).

Analysis of the single-twitch and tetanus experiments suggested minimal functional SR in our preparations, a nifedipine-sensitive LTCC contribution of minimal physiological relevance, and a continued and unimpeded Ca^{2+} source in the form of a rapidly activating current as detected in the unfused contractions during tetanus. However, the source of the majority of Ca^{2+} flux remains unidentified. We had previously demonstrated a regulatory role of taurine in cuttlefish systemic heart muscle contractility (MacCormack et al., 2016). To determine the effect of taurine on contractility, preparations were incubated in baths containing 100 mmol/L of either taurine or sucrose. Analysis of single-twitch contractile curve characteristics in mantle muscle preparations (Figure 5A) revealed that inclusion of exogenous taurine did not significantly impact peak stress (paired t test, Figure 5B, $p = .50$), change in impulse after 10 min (paired t test, Figure 5C, $p = .68$), peak stress production rate (paired t test, Figure 5D, $p = .67$), tetanus:twitch peak force ratio (paired t test, Figure 5E, $p = .36$), or magnitude of Fluo-4-coupled Ca^{2+} transients (paired t test, Figure 5F, $p = .37$).

Because we did not demonstrate sensitivity of contractility to taurine, and because functional characterization revealed no significant contribution of the SR to mantle contractility, we used TEM to examine the abundance and distribution of SR within muscle fibers of juvenile cuttlefish (Figure 6). The vast majority of intracellular space in myocytes was taken up by actomyosin structure, with nuclei and mitochondria relegated to the center of each cell, and with cells closely associated with thick collagen bundles (Figure 6A–D). The cross-sectional area of the SR was greatest at locations adjacent to the sarcolemmal membrane. Small-diameter SR tubules were observed across the rest of the fiber, but at low rates of occurrence. Most notably, highly structured and relatively extensive SR tubular aggregates (TAs) were found in the centers of multiple fibers (Figure 6E–H). These TAs were identified morphologically based on previous positive identifications of TAs colocalized with calsequestrin and the sarcoplasmic/endoplasmic calcium ATPase (SERCA) (Boncompagni et al., 2012).

4 | DISCUSSION

Cuttlefish are highly oxidative organisms (Capaz et al., 2017; Lamarre et al., 2016, 2019; Speers-Roesch et al., 2016), which, when combined with their high rates of growth (Sykes et al., 2014), are expected to undergo significant metabolic stress (i.e., high flux demand). In this study, the rate of protein synthesis in the mantle of 1-week-old cuttlefish (~0.2 g) was 2.5–3× higher than that of 1- and 2-month-old animals (~1–3 g). Protein synthesis incurs significant metabolic costs, because it requires a series of energy-intensive processes, including transcription, translation, and post-translational modifications, all of which demand a substantial amount of cellular resources and ATP equivalents. The rates of protein synthesis observed in the mantle of 1- and 2-month old animals are very similar to those observed in previous studies on animals of approximately the same size (Lamarre et al., 2019) and on much larger animals (~50 g) (Lamarre et al., 2016). The observed activity of CS, a qualitative indicator of mitochondrial capacity, in animals up to 3 g is fivefold higher than that found in 44-g cuttlefish (Speers-Roesch et al., 2016), consistent with the contention that small animals have high rates of oxidative metabolism (Speakman, 2005). This suggests that the first few weeks following hatching is a period of high flux demand in the life history of the organism. Moreover, low rates of HK activity, which is an index of glucose metabolism (0.25 $\mu mol \cdot min^{-1} \cdot g^{-1}$) in mantle relative to rates of oxygen consumption, reinforces a marked reliance on amino acid or lipid oxidation, as previously established (Lee, 1995). This interpretation is supported by a lack of glucose uptake in isolated mantle preparations. Even if only 10% of the measured tissue oxygen consumption rate was supported by glucose oxidation, glucose concentration in the extracellular medium after 1 h of incubation should be 0.90 mmol/L, easily detectable under the conditions tested. Low rates of glucose metabolism are also the case in larger animals (44 g) displaying similar rates of HK activity (0.1 $\mu mol \cdot min^{-1} \cdot g^{-1}$) (Speers-Roesch et al., 2016). Glucose uptake by mantle was not stimulated by taurine, as is the case in systemic heart from larger animals (~300 g) (MacCormack et al., 2016), suggesting either tissue or size and age specific differences in the regulatory role of taurine. Although glucose oxidation in mantle is not an important contributor to ATP production, a basal rate of metabolism appears to be critical, because impairment of glucose metabolism results in contractile failure, possibly related to disregulated levels of Na^+ and Ca^{2+} (Lamarre et al., 2019).

At high resting metabolic rates, additional activities, such as predation and predator avoidance, would exceed the animal's aerobic

17447410, 2024, 3, Downloaded from https://onlinelibrary.wiley.com/doi/10.1111/ivb.12439 by Universidade Do Algarve, Wiley Online Library on [06/11/2024]. See the Terms and Conditions (https://onlinelibrary.wiley.com/terms-and-conditions) on Wiley Online Library for rules of use; OA articles are governed by the applicable Creative Commons License

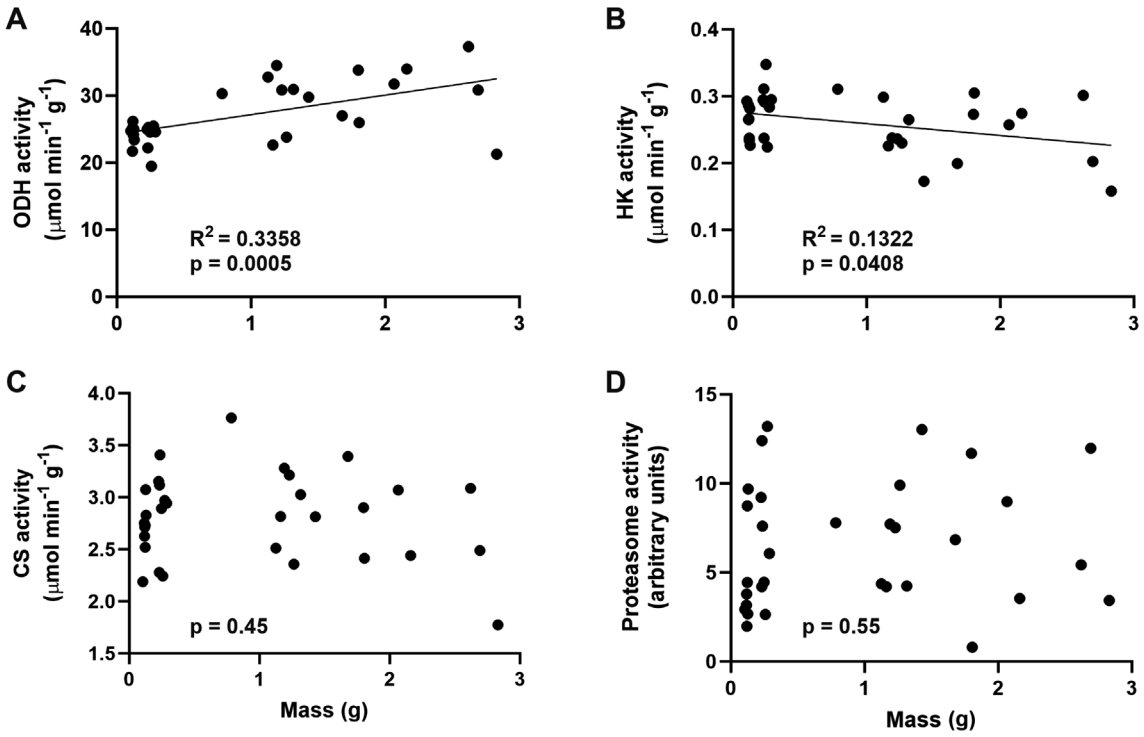

FIGURE 2 Mantle muscle enzyme activity in juvenile cuttlefish (*Sepia officinalis*). (A) Mantle octopine dehydrogenase (ODH) activity by whole-body mass. (B) Mantle hexokinase (HK) activity by whole-body mass. (C) Mantle citrate synthase (CS) activity by whole-body mass. (D) Mantle chymotrypsin-like 20S proteasome activity by whole-body mass. Regressions with slopes that significantly differed from zero are presented.

capacity and require anaerobic outlay. In cuttlefish, periods of heightened activity appear to result in a high NADH:NAD^+ ratio, which is rebalanced using ODH during rest (Capaz et al., 2017; Lamarre et al., 2019; Storey & Storey, 1979), and which would be in contrast to animals with sufficient aerobic scope to avoid incurring a metabolic debt. The activity of ODH reported here in cuttlefish <3 g body mass is similar to that in 44-g cuttlefish (Speers-Roesch et al., 2016), suggesting that anaerobic and aerobic metabolism do not scale in the same fashion over this size range. This interpretation is supported by findings that ODH activity in the mantle of squid, *Dosidicus gigas*, remains constant at body masses up to ~50 g and decreases at larger sizes (Trueblood & Seibel, 2014).

This high-flux metabolic physiology of juvenile cuttlefish may impose performance limitations and therefore force adaptation of the E–C coupling system that enables the mantle to function as a constant ventilatory pump and to power both sustained and burst swimming activity. These roles are in contrast to other aquatic species such as most fish, which ventilate with buccal and opercular muscles, and use red and white muscle for sustained aerobic and burst anaerobic swimming, respectively. In the current study, mass-specific metabolic rate decreased with animal mass (up to ~3 g), specific ODH activity increased, and specific HK activity decreased (Figure 2). These findings are consistent with the capacity of juvenile cuttlefish to rapidly incur a metabolic debt (Capaz et al., 2017; Lamarre et al., 2019; Storey & Storey, 1979). Correspondingly, mantle muscle preparations demonstrated robust single contractions but were unable to maintain baseline twitch stress in the subsequent contraction, let alone in a continued train (Figure 3). Indeed, behavioral studies have demonstrated exhaustion in cuttlefish after 5–30 s of jetting and a requirement for recovery periods lasting >1 h (Elder & Trueman, 1980). In mantle muscle preparations, these recovery periods are accompanied by a 30% increase in rates of tissue oxygen uptake (Lamarre et al., 2019), suggesting repeated contractions are fueled anaerobically.

In examining the link between metabolism and excitation–contraction coupling, we were unable to find ryanodine or nifedipine sensitivity in individual contractions, suggesting minimal SR and LTCC contributions to routine contractility. Tetanic contraction experiments (Figure 4) identified that a small but detectable nifedipine-sensitive LTCC current is present and that it is responsible for maintaining tetanus. However, the bulk of the tetanic stress, as well as the unfused contractions that captured ~50% of impulses at 50 Hz, was nifedipine-insensitive. Unfused contractions during tetanus indicate that Ca^{2+} cycling across the sarcolemmal or SR membrane is maintained at this high stimulation frequency. High-frequency, unfused contractions have been observed in prior studies on funnel retractor muscle of long-finned squid (*Doryteuthis pealeii*) (Rosenbluth et al., 2010) and *S. officinalis* (Lowy & Millman, 1962). We examined cells under TEM and found that much of the SR present in mantle myocytes was in the form of tubular aggregates. Tubular aggregates have been associated with loss of SR function, and their formation is generally attributed to oxidative stress (Boncompagni et al., 2012; Brady et al., 2016; Salviati et al., 1985).

17447410, 2024, 3, Downloaded from https://onlinelibrary.wiley.com/doi/10.1111/ivb.12439 by Universidade Do Algarve, Wiley Online Library on [06/11/2024]. See the Terms and Conditions (https://onlinelibrary.wiley.com/terms-and-conditions) on Wiley Online Library for rules of use; OA articles are governed by the applicable Creative Commons License

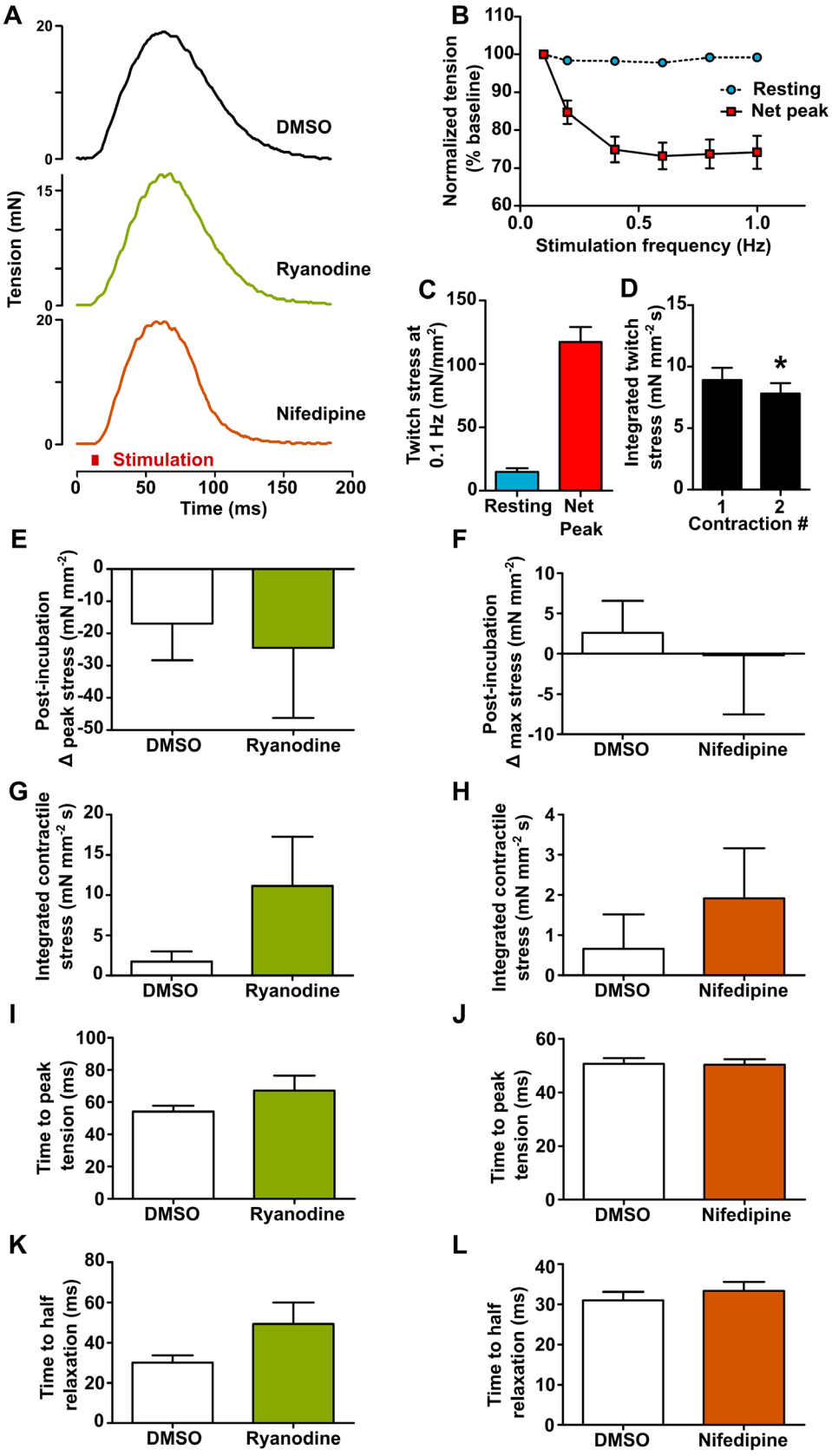

FIGURE 3 Sustained twitch endurance and contributors to $Ca2^{+}$ flux in isometrically contracting juvenile cuttlefish (*Sepia officinalis*) mantle muscle preparations. (A) Sample single stimulated (100 V, 0.2 Hz, 5 ms duration square waves) contractions in DMSO- sham-, ryanodine- (10 μmol/L), and nifedipine-treated (10 μmol/L) mantle preparations. (B) Relative force–frequency relationship within single preparations in resting (dotted, blue) and net peak (solid, red) tension, showing no summation between impulses ($n = 8$). (C) Absolute resting and peak stress at 0.2 Hz in DMSO-treated preparations ($n = 27$). (D) Time-integrated stresses significantly decrease in magnitude between the first and second successive contractions in the 6 × 0.2 Hz stimulation train ($n = 27$). (E) Effect of 10 μmol/L ryanodine (E, G, I, K) and 10 μmol/L nifedipine (F, H, J, L) on single mantle muscle stimulated contractions. Contractile parameters following a 10 min incubation period: change in peak stress (E, F), integrated contractile stress (G, H), and times from resting to peak tension (I, J) and from peak tension to half relaxation (K, L). Metrics are expressed as mean ± *SEM*; significance is indicated by * ($p < .05$).

This is internally consistent with the observed lack of ryanodine sensitivity and suggests a minimal contribution of SR Ca^{2+} cycling to myocyte contraction or relaxation.

In our previous work in both cuttlefish and fish, we found evidence that taurine regulates SL and SR Ca^{2+} cycling in heart (Gates et al., 2022; Henry & MacCormack, 2017; MacCormack

17447410, 2024, 3, Downloaded from https://onlinelibrary.wiley.com/doi/10.1111/ivb.12439 by Universidade Do Algarve, Wiley Online Library on [06/11/2024]. See the Terms and Conditions (https://onlinelibrary.wiley.com/terms-and-conditions) on Wiley Online Library for rules of use; OA articles are governed by the applicable Creative Commons License

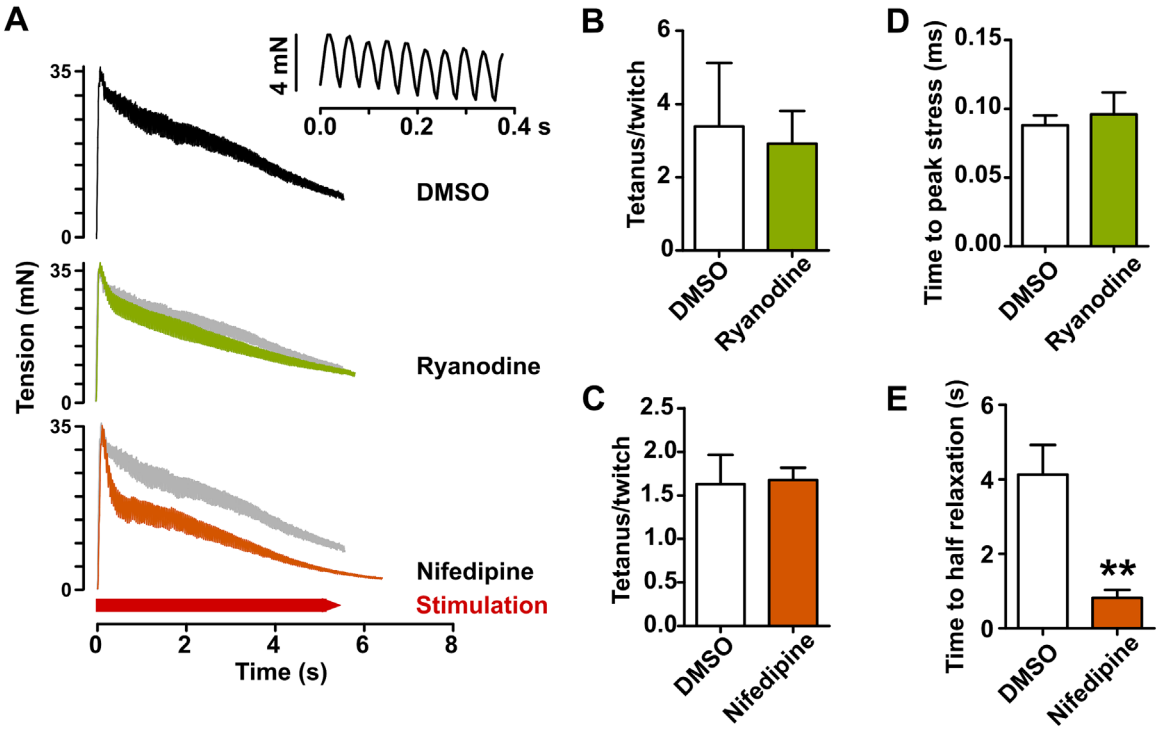

FIGURE 4 Analysis of isometric tetanic contractions in response to continuous stimulation (100 V, 50 Hz, 5 ms square wave pulses until 90% of peak stress dissipated) in juvenile cuttlefish (*Sepia officinalis*) mantle preparations. (A) Representative tetanic contractions in DMSO-, ryanodine- (10 μmol/L), and nifedipine-treated (10 μmol/L) mantle preparations ($n = 6$). Inset: representative oscillating subcontractions during 50 Hz simulation-induced tetanus in the DMSO treatment at ~25 Hz; these were observed in all samples. The DMSO sham sample trace is included in gray behind ryanodine- and nifedipine-treated sample traces. (B) Tetanus: twitch peak stress ratios between DMSO- and ryanodine-treated preparations. (C) Tetanus: twitch peak stress ratios between DMSO- and nifedipine-treated preparations. (D) Time to peak tetanic stress is not significantly different between paired DMSO- and ryanodine-treated samples. (E) Time from peak to half stress varies between DMSO- and nifedipine-treated preparations exposed to a tetanic stimulation. Bar graphs presented as mean ± *SEM*, significance is indicated by ** ($p < .01$).

et al., 2016). In the current model, no analogous sensitivity was noted, which is consistent with the lack of functional LTCC and SR under physiological conditions. The relative concentration of taurine in young versus adult mantle muscle remains unknown; because taurine is also known to support antioxidant function and regulation of glucose consumption (MacCormack et al., 2016), it may provide a means of regulating metabolic and contractile homeostasis as the animal grows.

These results demonstrate a decreased contribution of LTCCs to excitation-contraction coupling activity in juvenile *Sepia*, which is critical to the Ca^{2+}-dominated AP in adults as described previously (Rogers et al., 1997). If LTCCs are not the chief contributor to Ca^{2+} current (I_{Ca}), and thus the AP in juvenile cuttlefish mantle muscle, another voltage-gated Ca^{2+} channel would be the most obvious candidate to assume an analogous function. It is likely that the unidentified Ca^{2+} channel that is prominent in juvenile mantle is the source of the residual nifedipine-resistant Ca^{2+} flux found by Rogers et al. (1997). However, the route to positively identify the channel(s) implicated is made less clear because of established differences between invertebrate channel kinetics and their better understood mammalian counterparts. For example, a high-voltage-gated Ca^{2+} channel identified in freshwater snail (*Lymnaea* [= *Limnaea*] *stagnalis*) ganglia that shared mammalian N-type kinetics was nevertheless insensitive to nifedipine as well as to ω-conotoxin, a selective N-type blocker in mammals (Spafford et al., 2003); this activity was ablated with nonspecific Cd^{2+} administration. Similarly, low voltage-gated T-type channels have also been identified in *L. stagnalis* (Senatore & Spafford, 2010), and these channels shared more kinetic similarities with their mammalian analogs. The T-type current serves as a fast-depolarizing initiator to mammalian cardiac nodal APs, but is also known to drive I_{Ca}-dominant APs in the phyla Cnidaria, Mollusca, and Nematoda (reviewed by Smith et al., 2017). Finally, juvenile cuttlefish mantle muscle cells typically measured well under 5 μm in cross-sectional width (Figure 6), which likely prevents excessive Ca^{2+} diffusion limitation from the sarcolemma, as there is no evidence of a developed t-tubular system in squid striated muscle fibers of similar size (Kier, 1985). It is possible that the unknown Ca^{2+} channel provides the initial stimulus for the propagation of an AP (as in the T-type nodal role discussed above), which is then taken up by higher voltage-gated L-type channels to enhance the AP current and Ca^{2+} flux. As LTCC are often associated with t-tubules and potentially the peripheral coupling processes described by Kier (1985), their expression may be limited when such structures are underdeveloped. Alternatively, a faster and lower threshold current provided by a T-type channel or similar may prove advantageous in the reliable coordinated activation of the smaller

17447410, 2024, 3, Downloaded from https://onlinelibrary.wiley.com/doi/10.1111/ivb.12439 by Universidade Do Algarve, Wiley Online Library on [06/11/2024]. See the Terms and Conditions (https://onlinelibrary.wiley.com/terms-and-conditions) on Wiley Online Library for rules of use; OA articles are governed by the applicable Creative Commons License

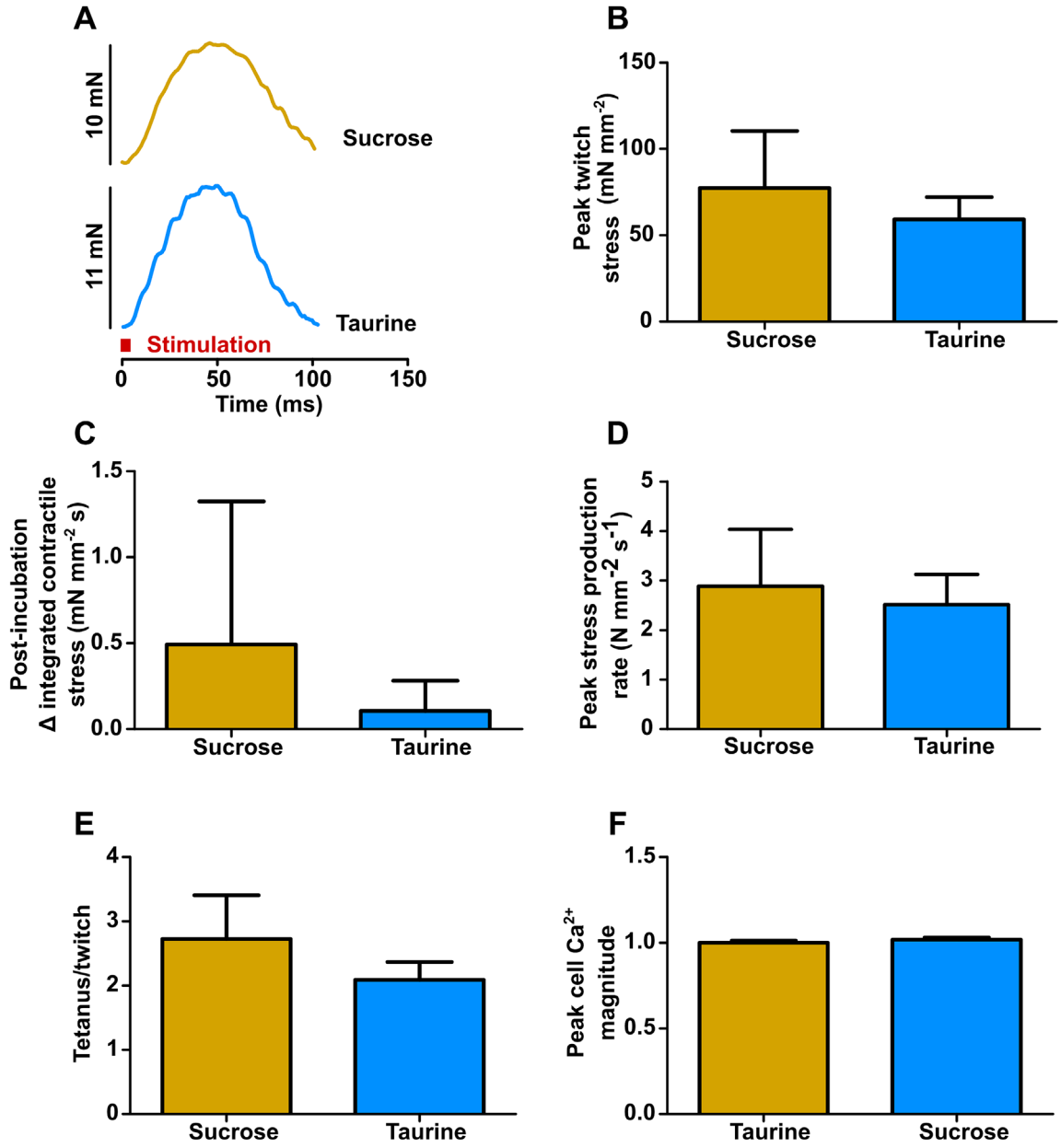

FIGURE 5 Twitch stress dependence on taurine in isometrically contracting juvenile cuttlefish (*Sepia officinalis*) mantle preparations. (A) Representative single-twitch contractile force curves of isometrically contracting mantle muscle preparations treated with 100 mmol/L sucrose or taurine. Treatments were compared for peak single twitch stress (B), pre- to post-10-min incubation time-integrated twitch stress (C), maximum stress production rate (D), tetanus:twitch peak force ratio (E), and single-cell fluorescent Ca^{2+} transient magnitude (F). There was no significant difference ($p < .05$) in any parameter assessed; $n = 7$ paired preparations; in panel F, cells from $n = 3$ animals per treatment were analyzed.

muscle fibers; this coordination could become less effective as larger fibers become predominant with animal size.

In young coleoids, high-frequency, high-volume, and low-velocity jetting is the preferable means of transportation because of the mechanical disadvantage of undulatory swimming at low to intermediate Reynolds' numbers (*Re*) (Bartol et al., 2008, 2009). This is reflected in the differential power curve and faster contraction–relaxation kinetics in juvenile versus adult cuttlefish (Gladman & Askew, 2022). Lower threshold Ca^{2+} channels with faster activation–deactivation kinetics would also provide an advantage with respect to cycling frequency. However, the use of fast-cycling channels may impose a physiological challenge in the form of accumulating intracellular Ca^{2+} (Ca^{2+}_i), which may both limit full contractility and impose cytotoxicity (Boncompagni et al., 2012). The appearance of TAs may represent a physiological means of clearing Ca^{2+}_i to maintain contractility and electrophysiological homeostasis. As the animal grows, *Re* increases, and metabolic demands decrease; we might expect to see a transition toward an adult phenotype in E–C coupling, combined with a shift in SR and LTCC predominance. It is conceivable that SR de-aggregation or cardiac remodeling could

17447410, 2024, 3, Downloaded from https://onlinelibrary.wiley.com/doi/10.1111/ivb.12439 by Universidade Do Algarve, Wiley Online Library on [06/11/2024]. See the Terms and Conditions (https://onlinelibrary.wiley.com/terms-and-conditions) on Wiley Online Library for rules of use; OA articles are governed by the applicable Creative Commons License

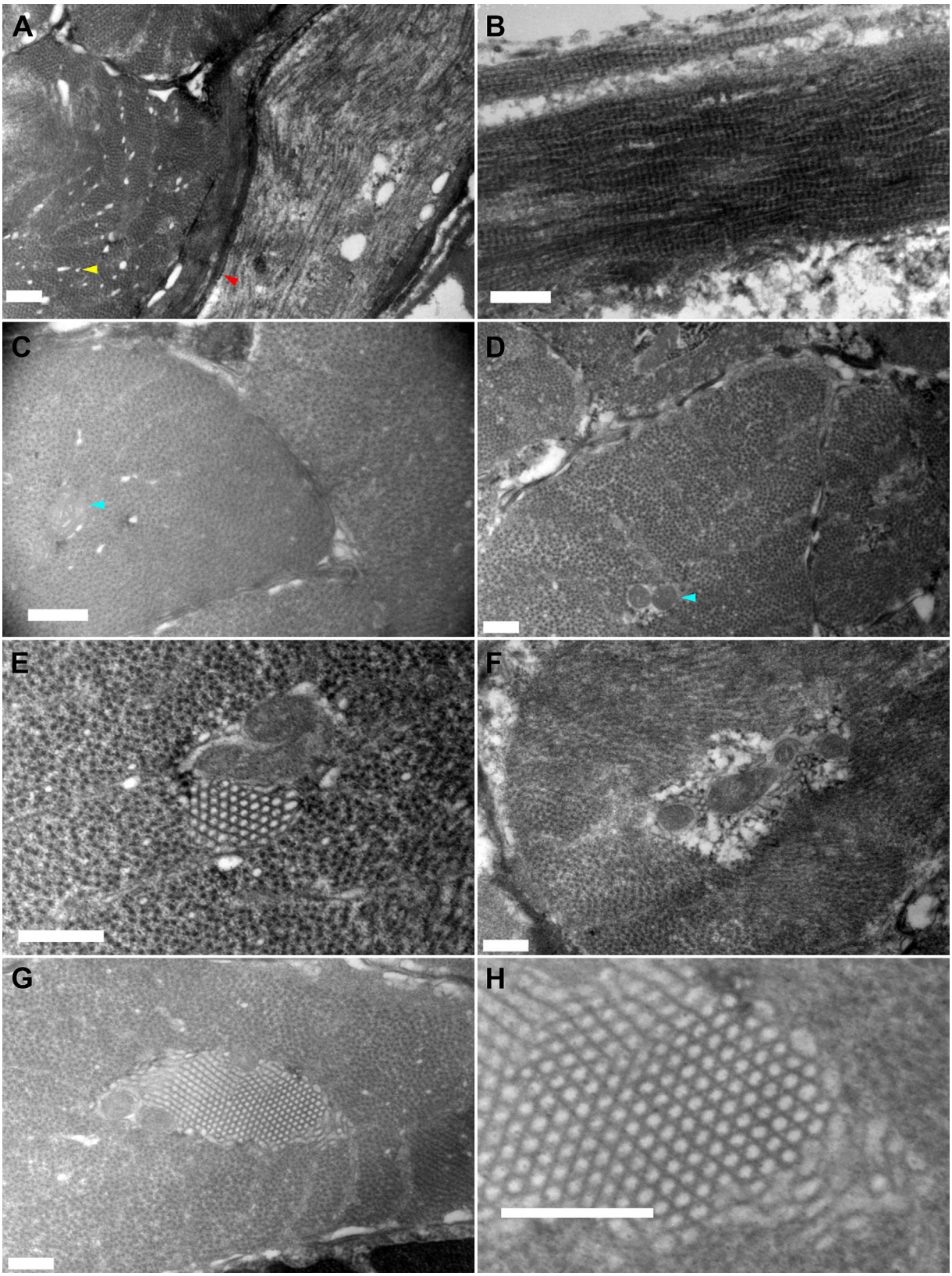

FIGURE 6 Cross-sectional TEM of circumferential mantle sections from juveniles of *Sepia officinalis*, oriented with circumferential fibers emerging from the page (from $n = 2$ preparations). (A) Interface between orthogonal muscle fibers, separated by fascia (red arrowhead). Peripheral and central sarcoplasmic reticulum (SR; yellow arrowhead) content is minimal. The longitudinal muscle fiber here is obliquely striated. (B) Putative collagen bundle, oriented orthogonally to the circumferential fibers. (C, D) Circumferential, obliquely striated fiber bundles, with myosin uniformly in-phase. Each cell tends to maintain mitochondria (blue arrowhead) solely in the center of the cell, with very little boundary or central SR. (E–G) Extensive SR tubular aggregates (TAs) found in the center of different cells. (H) Fine detail of SR aggregate in G, showing less-organized SR at the boundaries of the highly ordered aggregate. All scale bars = 500 nm.

17447410, 2024, 3, Downloaded from https://onlinelibrary.wiley.com/doi/10.1111/ivb.12439 by Universidade Do Algarve, Wiley Online Library on [06/11/2024]. See the Terms and Conditions (https://onlinelibrary.wiley.com/terms-and-conditions) on Wiley Online Library for rules of use; OA articles are governed by the applicable Creative Commons License

lead to an active SR contribution that may inversely mirror the whole-animal decrease in $\dot{M}O_2$ (Johansen et al., 1982; Lamarre et al., 2019), as well as a switch to the LTCC-dominant AP demonstrated by Rogers.

In conclusion, we describe the coordinated energetics enabling E–C coupling in mantle muscle of juvenile cuttlefish during a period of very high metabolic demand in the organism's life history. We demonstrate exceptionally high rates of protein synthesis in the mantle of animals <0.5 g along with minimal reliance on glucose oxidation. Mantle muscle from juvenile cuttlefish demonstrated minimal SR and LTCC contributions to contractility, exhibiting SR in the form of tubular aggregates. In marked contrast to the systemic heart in adult cuttlefish, extracellular taurine did not influence either contractile function or glucose utilization. We postulate that the energetics of mantle muscle are well suited to the mechanical environment of young animals, and correlate to the kinetics of the as-yet unidentified sarcolemmal Ca^{2+} source.

AUTHOR CONTRIBUTIONS

The study was conceived, designed, and executed by Neal I. Callaghan, Simon G. Lamarre, Loïck Ducros, J. Craig Bennett, José Pedro Andrade, William R. Driedzic, and Tyson J. MacCormack. Juan C. Capaz and Antonio V. Sykes performed the animal husbandry.

ACKNOWLEDGMENTS

The authors wish to thank João Reis and the staff at CCMAR Ramalhete for their assistance with the study.

CONFLICT OF INTEREST STATEMENT

The authors declare that the research was conducted in the absence of any commercial or financial relationships that could be construed as a potential conflict of interest.

DATA AVAILABILITY STATEMENT

The data that support the findings of this study are available from the corresponding author upon reasonable request.

ORCID

Neal I. Callaghan https://orcid.org/0000-0001-8214-3395
Simon G. Lamarre https://orcid.org/0000-0001-7038-4626

REFERENCES

Altimiras, J., Hove-Madsen, L., & Gesser, H. (1999). Ca(2+) uptake in the sarcoplasmic reticulum from the systemic heart of octopod cephalopods. *Journal of Experimental Biology*, *202*(Pt 18), 2531–2537. http://www.ncbi.nlm.nih.gov/pubmed/10460740, https://doi.org/10.1242/jeb.202.18.2531

Bartol, I. K., Krueger, P. S., Stewart, W. J., & Thompson, J. T. (2009). Pulsed jet dynamics of squid hatchlings at intermediate Reynolds numbers. *Journal of Experimental Biology*, *212*(10), 1506–1518. https://doi.org/10.1242/jeb.026948

Bartol, I. K., Krueger, P. S., Thompson, J. T., & Stewart, W. J. (2008). Swimming dynamics and propulsive efficiency of squids throughout ontogeny. *Integrative and Comparative Biology*, *48*(6), 720–733. https://doi.org/10.1093/icb/icn043

Bers, D. M. (1989). SR Ca loading in cardiac muscle preparations based on rapid-cooling contractures. *American Journal of Physiology-Cell Physiology*, *256*(1), C109–C120. https://doi.org/10.1152/ajpcell.1989.256.1.C109

Boncompagni, S., Protasi, F., & Franzini-Armstrong, C. (2012). Sequential stages in the age-dependent gradual formation and accumulation of tubular aggregates in fast twitch muscle fibers: SERCA and calsequestrin involvement. *Age*, *34*(1), 27–41. https://doi.org/10.1007/s11357-011-9211-y

Brady, S., Healy, E. G., Gang, Q., Parton, M., Quinlivan, R., Jacob, S., Curtis, E., Al-Sarraj, S., Sewry, C. A., Hanna, M. G., Houlden, H., Beeson, D., & Holton, J. L. (2016). Tubular aggregates and cylindrical spirals have distinct immunohistochemical signatures. *Journal of Neuropathology & Experimental Neurology*, *75*(12), 1171–1178. https://doi.org/10.1093/jnen/nlw096

Capaz, J. C., Tunnah, L., MacCormack, T. J., Lamarre, S. G., Sykes, A. V., & Driedzic, W. R. (2017). Hypoxic induced decrease in oxygen consumption in cuttlefish (*Sepia officinalis*) is associated with minor increases in mantle octopine but no changes in markers of protein turnover. *Frontiers in Physiology*, *8*(MAY), 344. https://doi.org/10.3389/fphys.2017.00344

Dabrowski, K. (1978). The density and chemical composition of fish muscle. *Experientia*, *34*(10), 1263–1265. https://doi.org/10.1007/BF01981406

Elder, H. Y., & Trueman, E. R. (1980). Swimming by jet propulsion. In *Aspects of animal movement*. Cambridge University Press.

Feinstein, N., Nesher, N., & Hochner, B. (2011). Functional morphology of the neuromuscular system of the *Octopus vulgaris* arm. *Vie et Milieu - Life and Environment*, *61*(4), 219–229.

Fiorito, G., Affuso, A., Basil, J., Cole, A., de Girolamo, P., D'Angelo, L., Dickel, L., Gestal, C., Grasso, F., Kuba, M., Mark, F., Melillo, D., Osorio, D., Perkins, K., Ponte, G., Shashar, N., Smith, D., Smith, J., & Andrews, P. L. (2015). Guidelines for the care and welfare of cephalopods in research—A consensus based on an initiative by CephRes, FELASA and the Boyd Group. *Laboratory Animals*, *49*(2_suppl), 1–90. https://doi.org/10.1177/0023677215580006

Fraser, K. P. P., & Rogers, A. D. (2007). Protein metabolism in marine animals: The underlying mechanism of growth. *Advances in Marine Biology*, *52*, 267–362. https://doi.org/10.1016/S0065-2881(06)52003-6

Garlick, P. J., McNurlan, M. A., & Preedy, V. R. (1980). A rapid and convenient technique for measuring the rate of protein synthesis in tissues by injection of [3H]phenylalanine. *Biochemical Journal*, *192*(2), 719–723. https://doi.org/10.1042/bj1920719

Gates, M. A., Morash, A. J., Lamarre, S. G., & MacCormack, T. J. (2022). Intracellular taurine deficiency impairs cardiac contractility in rainbow trout (*Oncorhynchus mykiss*) without affecting aerobic performance. *Journal of Comparative Physiology B*, *192*(1), 49–60. https://doi.org/10.1007/s00360-021-01407-4

Gesser, H., Driedzic, W. R., Rantin, F. T., & de Freitas, J. C. (1997). Ca2+ regulation of heart contractility in *Octopus*. *Journal of Comparative Physiology B*, *167*(7), 474–480. https://doi.org/10.1007/s003600050099

Gissel, H. (2005). The role of Ca2+ in muscle cell damage. *Annals of the new York Academy of Sciences*, *1066*(1), 166–180. https://doi.org/10.1196/annals.1363.013

Gladman, N. W., & Askew, G. N. (2022). The mechanical properties of the mantle muscle of European cuttlefish (*Sepia officinalis*). *Journal of Experimental Biology*, *225*(23), jeb244977. https://doi.org/10.1242/jeb.244977

Henry, E. F., & MacCormack, T. J. (2017). Taurine protects cardiac contractility in killifish, *Fundulus heteroclitus*, by enhancing sarcoplasmic reticular Ca2+ cycling. *Journal of Comparative Physiology B*, *188*(1), 89–99. https://doi.org/10.1007/s00360-017-1107-4

17447410, 2024, 3, Downloaded from https://onlinelibrary.wiley.com/doi/10.1111/ivb.12439 by Universidade Do Algarve, Wiley Online Library on [06/11/2024]. See the Terms and Conditions (https://onlinelibrary.wiley.com/terms-and-conditions) on Wiley Online Library for rules of use; OA articles are governed by the applicable Creative Commons License

Johansen, K., Brix, O., & Lykkeboe, G. (1982). Blood gas transport in the cephalopod, *Sepia officinalis*. *The Journal of Experimental Biology*, *99*, 331–338. https://doi.org/10.1242/jeb.99.1.331

Kier, W. M. (1985). The musculature of squid arms and tentacles: Ultrastructural evidence for functional differences. *Journal of Morphology*, *185*(2), 223–239. https://doi.org/10.1002/jmor.1051850208

Konishi, M., Kurihara, S., & Sakai, T. (1985). Change in intracellular calcium ion concentration induced by caffeine and rapid cooling in frog skeletal muscle fibres. *Journal of Physiology*, *365*, 131–146. https://doi.org/10.1113/jphysiol.1985.sp015763

Lamarre, S. G., Ditlecadet, D., McKenzie, D. J., Bonnaud, L., & Driedzic, W. R. (2012). Mechanisms of protein degradation in mantle muscle and proposed gill remodeling in starved *Sepia officinalis*. *American Journal of Physiology. Regulatory, Integrative and Comparative Physiology*, *303*(4), R427–R437. https://doi.org/10.1152/ajpregu.00077.2012

Lamarre, S. G., MacCormack, T. J., Bourloutski, É., Callaghan, N. I., Pinto, V. D., Andrade, J. P., Sykes, A. V., & Driedzic, W. R. (2019). Interrelationship between contractility, protein synthesis and metabolism in mantle of juvenile cuttlefish (*Sepia officinalis*). *Frontiers in Physiology*, *10*, 1051. https://doi.org/10.3389/fphys.2019.01051

Lamarre, S. G., MacCormack, T. J., Sykes, A. V., Hall, J. R., Speers-Roesch, B., Callaghan, N. I., & Driedzic, W. R. (2016). Metabolic rate and rates of protein turnover in food-deprived cuttlefish, *Sepia officinalis* (Linnaeus 1758). *American Journal of Physiology - Regulatory, Integrative and Comparative Physiology*, *310*(11), R1160–R1168. https://doi.org/10.1152/ajpregu.00459.2015

Lamarre, S. G., Saulnier, R. J., Blier, P. U., & Driedzic, W. R. (2015). A rapid and convenient method for measuring the fractional rate of protein synthesis in ectothermic animal tissues using a stable isotope tracer. *Comparative Biochemistry and Physiology Part B*, *182*, 1–5. https://doi.org/10.1016/j.cbpb.2014.11.006

Layland, J., Young, I. S., & Altringham, J. D. (1995). The effect of cycle frequency on the power output of rat papillary muscles *in vitro*. *The Journal of Experimental Biology*, *198*(Pt 4), 1035–1043. http://www.ncbi.nlm.nih.gov/pubmed/7730751, https://doi.org/10.1242/jeb.198.4.1035

Lee, P. G. (1995). Nutrition of cephalopods: Fueling the system. *Marine and Freshwater Behaviour and Physiology*, *25*(1–3), 35–51. https://doi.org/10.1080/10236249409378906

Lewbart, G. A., & Mosley, C. (2012). Clinical anesthesia and analgesia in invertebrates. *Journal of Exotic Pet Medicine*, *21*(1), 59–70. https://doi.org/10.1053/j.jepm.2011.11.007

Lowy, J., & Millman, B. M. (1962). Mechanical properties of smooth muscles of cephalopod molluscs. *The Journal of Physiology*, *160*(2), 353–363. https://doi.org/10.1113/jphysiol.1962.sp006850

MacCormack, T. J., Callaghan, N. I., Sykes, A. V., & Driedzic, W. R. (2016). Taurine depresses cardiac contractility and enhances systemic heart glucose utilization in the cuttlefish, *Sepia officinalis*. *Journal of Comparative Physiology B*, *186*(2), 215–227. https://doi.org/10.1007/s00360-015-0946-0

Milligan, B. J., Curtin, N. A., & Bone, Q. (1997). Contractile properties of obliquely striated muscle from the mantle of squid (*Alloteuthis subulata*) and cuttlefish (*Sepia officinalis*). *The Journal of Experimental Biology*, *200*, 2425–2436. http://www.ncbi.nlm.nih.gov/pubmed/9320349, https://doi.org/10.1242/jeb.200.18.2425

Packard, A., & Trueman, E. R. (1974). Muscular activity of the mantle of *Sepia* and *Loligo* (Cephalopoda) during respiratory movements and jetting, and its physiological interpretation. *The Journal of Experimental Biology*, *61*(2), 411–419. http://jeb.biologists.org/content/61/2/411.abstract, https://doi.org/10.1242/jeb.61.2.411

Rogers, C., Nelson, L., Milligan, B. J., & Brown, E. R. (1997). Different excitation-contraction coupling mechanisms exist in squid, cuttlefish and octopod mantle muscle. *The Journal of Experimental Biology*, *200*, 3033–3041. http://www.ncbi.nlm.nih.gov/pubmed/9359892, https://doi.org/10.1242/jeb.200.23.3033

Rosenbluth, J., Szent-Gyorgyi, A. G., & Thompson, J. T. (2010). The ultrastructure and contractile properties of a fast-acting, obliquely striated, myosin-regulated muscle: The funnel retractor of squids. *Journal of Experimental Biology*, *213*(14), 2430–2443. https://doi.org/10.1242/jeb.037820

Salviati, G., Pierobon-Bormioli, S., Betto, R., Damiani, E., Angelini, C., Ringel, S. P., Salvatori, S., & Margreth, A. (1985). Tubular aggregates: Sarcoplasmic reticulum origin, calcium storage ability, and functional implications. *Muscle & Nerve*, *8*(4), 299–306. http://www.ncbi.nlm.nih.gov/pubmed/16758596, https://doi.org/10.1002/mus.880080406

Senatore, A., & Spafford, J. D. (2010). Transient and big are key features of an invertebrate T-type channel (LCav3) from the central nervous system of *Lymnaea stagnalis*. *Journal of Biological Chemistry*, *285*(10), 7447–7458. https://doi.org/10.1074/jbc.M109.090753

Shibatani, T., & Ward, W. F. (1995). Sodium dodecyl sulfate (SDS) activation of the 20S proteasome in rat liver. *Archives of Biochemistry and Biophysics*, *321*(1), 160–166. https://doi.org/10.1006/abbi.1995.1381

Shiels, H. A., Santiago, D. A., & Galli, G. L. J. (2010). Hypercapnic acidosis reduces contractile function in the ventricle of the armored catfish, *Pterygoplichthys pardalis*. *Physiological and Biochemical Zoology*, *83*(2), 366–375. https://doi.org/10.1086/644759

Smith, C. L., Abdallah, S., Wong, Y. Y., Le, P., Harracksingh, A. N., Artinian, L., Tamvacakis, A. N., Rehder, V., Reese, T. S., & Senatore, A. (2017). Evolutionary insights into T-type Ca(2+) channel structure, function, and ion selectivity from the *Trichoplax adhaerens* homologue. *The Journal of General Physiology*, *149*(4), 483–510. https://doi.org/10.1085/jgp.201611683

Spafford, J. D., Chen, L., Feng, Z., Smit, A. B., & Zamponi, G. W. (2003). Expression and modulation of an invertebrate presynaptic calcium channel α1 subunit homolog. *Journal of Biological Chemistry*, *278*(23), 21178–21187. https://doi.org/10.1074/jbc.M302212200

Speakman, J. R. (2005). Body size, energy metabolism and lifespan. *Journal of Experimental Biology*, *208*(9), 1717–1730. https://doi.org/10.1242/jeb.01556

Speers-Roesch, B., Callaghan, N. I., MacCormack, T. J., Lamarre, S. G., Sykes, A. V., & Driedzic, W. R. (2016). Enzymatic capacities of metabolic fuel use in cuttlefish (Sepia officinalis) and responses to food deprivation: Insight into the metabolic organization and starvation survival strategy of cephalopods. *Journal of Comparative Physiology B*, *186*(6), 711–725. https://doi.org/10.1007/s00360-016-0991-3

Staaf, D. J., Gilly, W. F., & Denny, M. W. (2014). Aperture effects in squid jet propulsion. *Journal of Experimental Biology*, *217*(9), 1588–1600. https://doi.org/10.1242/jeb.082271

Storey, K. B., & Storey, J. M. (1979). Octopine metabolism in the cuttlefish, *Sepia officinalis*: Octopine production by muscle and its role as an aerobic substrate for non-muscular tissues. *Journal of Comparative Physiology B*, *131*(4), 311–319. https://doi.org/10.1007/BF00688806

Sykes, A. V., Domingues, P., & Andrade, J. P. (2014). Sepia officinalis. In J. Iglesias, L. Fuentes, & R. Villanueva (Eds.), *Cephalopod culture* (pp. 175–204). Springer. https://doi.org/10.1007/978-94-017-8648-5_11

Talon, S., Huchet-Cadiou, C., & Léoty, C. (2000). Rapid cooling-induced contractures in rat skinned skeletal muscle fibres originate from sarcoplasmic reticulum Ca2+ release through ryanodine and inositol trisphosphate receptors. *Pflügers Archiv*, *441*(1), 108–117. https://doi.org/10.1007/s004240000375

Trueblood, L. A., & Seibel, B. A. (2014). Slow swimming, fast strikes: Effects of feeding behavior on scaling of anaerobic metabolism in epipelagic squid. *The Journal of Experimental Biology*, *217*(15), 2710–2716. https://doi.org/10.1242/jeb.106872

Trueman, E. R., & Packard, A. (1968). Motor performances of some cephalopods. *The Journal of Experimental Biology*, *49*(3), 495–507. http://jeb.

17447410, 2024, 3, Downloaded from https://onlinelibrary.wiley.com/doi/10.1111/ivb.12439 by Universidade Do Algarve, Wiley Online Library on [06/11/2024]. See the Terms and Conditions (https://onlinelibrary.wiley.com/terms-and-conditions) on Wiley Online Library for rules of use; OA articles are governed by the applicable Creative Commons License

biologists.org/content/49/3/495.abstract, https://doi.org/10.1242/jeb.49.3.495

Vidal, E. A. G., & Shea, E. K. (2023). Cephalopod ontogeny and life cycle patterns. *Frontiers in Marine Science*, *10*(July), 1–24. https://doi.org/10.3389/fmars.2023.1162735

Zullo, L., Fossati, S. M., Imperadore, P., & Nödl, M.-T. (2017). Molecular determinants of cephalopod muscles and their implication in muscle regeneration. *Frontiers in Cell and Developmental Biology*, *5*, 53. https://doi.org/10.3389/fcell.2017.00053

How to cite this article: Callaghan, N. I., Ducros, L., Bennett, J. C., Capaz, J. C., Andrade, J. P., Sykes, A. V., Driedzic, W. R., Lamarre, S. G., & MacCormack, T. J. (2024). Excitation–contraction coupling reflects the metabolic profile of mantle muscle in young cuttlefish (*Sepia officinalis*). *Invertebrate Biology*, *143*(3), e12439. https://doi.org/10.1111/ivb.12439

17447410, 2024, 3, Downloaded from https://onlinelibrary.wiley.com/doi/10.1111/ivb.12439 by Universidade Do Algarve, Wiley Online Library on [06/11/2024]. See the Terms and Conditions (https://onlinelibrary.wiley.com/terms-and-conditions) on Wiley Online Library for rules of use; OA articles are governed by the applicable Creative Commons License